01 Jan 2004

Cause and Effects of Voltage Collapse -- Case Studies with Dynamic Simulations

Feng Dong

Mariesa Crow
Missouri University of Science and Technology, crow@mst.edu

Badrul H. Chowdhury
Missouri University of Science and Technology, bchow@mst.edu

Levent Acar
Missouri University of Science and Technology, acar@mst.edu

Recommended Citation

F. Dong et al., "Cause and Effects of Voltage Collapse -- Case Studies with Dynamic Simulations," *Proceedings of the IEEE Power Engineering Society General Meeting (2004, Denver, Colorado)*, vol. 2, pp. 1806-1812, Institute of Electrical and Electronics Engineers (IEEE), Jan 2004.
The definitive version is available at https://doi.org/10.1109/PES.2004.1373191

Cause and Effects of Voltage Collapse – Case Studies with Dynamic Simulations

Feng Dong[1], *Student member, IEEE*
Badrul H. Chowdhury, *Senior Member, IEEE*
Mariesa Crow, *Senior Member, IEEE*
Levent Acar, *Senior Member, IEEE*

Abstract-- **Voltage collapse studies are made to gain an insight into mechanisms that drive a system into collapse. The inter-play of generator controls in local and external areas are explored. Simulations are carried out on a medium sized network by a transient dynamic simulation program. Simulation results help to better understand remediation strategies. The time dependent characteristics of corrective controls are investigated.**

Index terms – **Load tap changer, over excitation limiter, reactive power margin, stability margin, preventive control.**

I. INTRODUCTION

The voltage stability problem in power systems is attracting more attention from researchers around the world mainly because of several voltage collapse incidents in recent history [1]. It is widely felt that the uncertainties of power system restructuring efforts as well as utility economics have led many companies to operate their systems close to the maximum loadability limits thereby unwittingly pushing their systems toward the brink of collapse. There are several definitions of voltage stability. One definition developed by CIGRE is that at a operating condition and subject to a disturbance the system is voltage stability if voltages at load buses approach their post-disturbance equilibrium points [7].

The analysis methods for voltage stability problems are classified into two classes, static and dynamic analysis. Several well known static methods are based on sensitivity factors such as $\partial V / \partial Q$; eigenvalues and singular values; and continuation power flow [2, 3]. These power flow-based static methods can provide a measure of the degree of stability, like a proximity indicator, dominant eigenvalues, real and reactive power margins, etc. Dynamic simulations, on the other hand, can reproduce the time response of the system to a sequence of discrete events. Therefore, it is able to shed light on the mechanism of voltage stability and also provide corrective strategies to improve voltage stability [4, 5].

Voltage collapse, though uncommon, can occur as the consequence of interactions among all fast and slow dynamics in power systems, especially reactive generation and consumption equipment. A possible sequence of events leading up to a collapse could be the following: a critical disturbance occurs or a critical load increases; voltages at load buses drop steeply; generator AVRs reacting to lowered terminal voltages demand higher field currents to produce additional reactive power to boost up the voltages; load bus voltages continue to drop; the under load tap changers (ULTC) attempt to restore voltages after an initial time delay; reactive reserves at certain sensitive generators approach their individual limits, such as the over excitation limit (OEL) or, worse, the armature current limit (ACL); area-wide bus voltages decline precipitously; finally the system collapses. As obvious, many factors have to coincide and events have to occur simultaneously for a collapse process to initiate. In this paper, we revisit the collapse mechanism with the help of a commercial transient simulation program EUROSTAG [6]. The intent is to answer the following questions:

1. What are the driving forces of voltage stability? How does real and reactive power change during system dynamics leading to voltage instability?
2. Is reactive control of generators local or system-wide? What role do weak areas within a large scale system play? How do the weak areas evolve during collapse?
3. Are the results of static analysis consistent with those from dynamic simulations?
4. How do control actions of ULTC and generator limiters impact voltage stability?
5. Are shunt switch capacitors effective in remediating voltage collapse?

In the next section some important models are presented. The dynamics of reactive power generations and loads are investigated. A case study is performed in Section III and discussions are made in the context of the above questions.

II. SYSTEM MODEL

The power system is modeled as a set of algebraic-differential equations.

$$0 = g(x, y) \tag{1}$$

$$\dot{x} = f(x, y) \tag{2}$$

Where x are the state variables, and y are the algebraic variables, usually bus voltages.

1) Load model

Voltage-sensitive loads can be modeled as [7]:

$$P_{load} = P_0 (\frac{V}{V_0})^{\beta} \tag{3}$$

$$Q_{load} = Q_0 (\frac{V}{V_0})^{\eta} \tag{4}$$

This work was supported in part by the U.S. Natioal Science Foundation under Grant ECS-9975713.

[1]F. Dong (email: fd2h3@umr.edu), B. H. Chowdhury (email: bchow@ece.umr.edu), M. L.Crow (email: crow@ece.umr.edu), and L. Acar (email acar@ece.umr.edu) are with the Electrical & Computer Engineering Department at the University of Missouri-Rolla, Rolla, MO 65409.

where P_0 is the real power at V=1.0 pu, Q_0 is the reactive power at V=1.0 pu, V is the bus voltage magnitude, β is the voltage sensitivity exponent of the real power, and η is the voltage sensitivity exponent of the reactive power.

Thus, with $\beta = 2$, and $\eta = 2$, the load becomes a constant impedance type. Dynamic loads are modeled as induction motors. The load at one node can be represented as a combination of different kinds of loads, e.g. one portion of the load is consumed by an impedance load and the rest could be modeled as dynamic induction motor loads.

2) Generator modeling

Several different types of exciters may be installed within a system, such as the DC1A, ST1A, ST3A etc. Some generators may be equipped with PSS, and a turbine/governor sub-system.

3) ULTC model

A ULTC can automatically adjust and keep the load-side bus voltage constant given that enough buck or boost taps exist. A model of the ULTC is shown as follows [7]:

$$n_{k+1} = n_k - df(V - V_{set}) \tag{5}$$

where: d is the step size of the transformer;

n is the turn ratio; and

$$f(x) = \begin{cases} -1 & \text{if} \quad x \le -\varepsilon \ ; \\ 0 & \text{if} \ |x| < \varepsilon \ ; \\ 1 & \text{if} \quad x \ge \varepsilon . \end{cases} \tag{6}$$

Time delays of ULTC action at the first instance is usually much longer than the time delays associated with successive actions of the ULTC. Each ULTC has finite (usually 32) taps and step size is usually 0.000625.

III. Case Study

A reduced WSCC system is studied for this paper. This system contains 283 buses, 407 branches and transformers. There are 29 generators and 103 loads. Generators are located at buses 105, 106, 112, 116, 118, 138, 144 and 148. Summed type OELs are installed at generator buses 118, 144 and 148. The system is composed of several sub-areas, namely BC, WA, MT, ID, WY, UT, OR, CO, NM, NV, AZ, CA. The heavy loads are concentrated in California (CA) for the particular season studied. Certain sub-areas such as WA, MT etc. are responsible for supplying the bulk of the power to CA mostly via 500 kV lines. Each load at the 103 load buses is fed by a ULTC. The time delays of the ULTCs are set to 80s for the action and 5s between successive actions. The simplified system diagram is provided in Fig. A1 in the Appendix.

A. The scenario

At initial operating condition, the total generation is 61422 MW and 17742 MVar. The total system load is 60785 MW and 7940. As shown in Fig. A1, the CA sub-area located at the lower left of the system diagram, is heavily loaded. In this sub-area, the generation and load are respectively (12603 + j4727) and (13765+j4543) and the real power import from other sub-areas is 1100 MW. The total loads consist of 50% impedance loads and 50% induction motor load. The larger induction motors are located at buses 1119, 1109 and 1142. The disturbance consists of two lines between 76 and 82 disconnected out of service. Initially about 900 MW power is delivered from BC sub-area at the top of the WSCC system to CA. The first transmission line is switched out at 10 seconds and the second line at 30s.

B. Dynamic simulations

The voltage profiles at buses 118 and 100 are shown in Fig. 1. Voltages drop at 10s and 30s corresponding to the above events. At 25s and 50s second time instant respectively, the OELs at generators 144 and 148 are enforced first, then at 70s, the OEL at generator 118 is engaged (the parameters are deliberately set to make OELs act fast). When generator 118 reaches its field current limit, it losses voltage control capability and this leads to a large reduction of terminal voltage as shown in curve 'v118'. Although these limiters are engaged to constrain reactive power generation, they do not lead to system collapse. After 80 seconds time delay, ULTCs start to restore voltages and loads. The system becomes stressed even further and eventually collapses at 150 sec.

TABLE 1. EVENT LIST

TIME	EVENT
10	The first Line 76-82 is tripped off
25	OEL at Gen 144 is enforced
40	The second line 76-82 is opened
50	OEL at Gen 148 is enforced
70	OEL at Gen 118 engages
80	Most ULTCs in CA area begin to operate
147	Induction motor 1148 stalls
150	System collapses

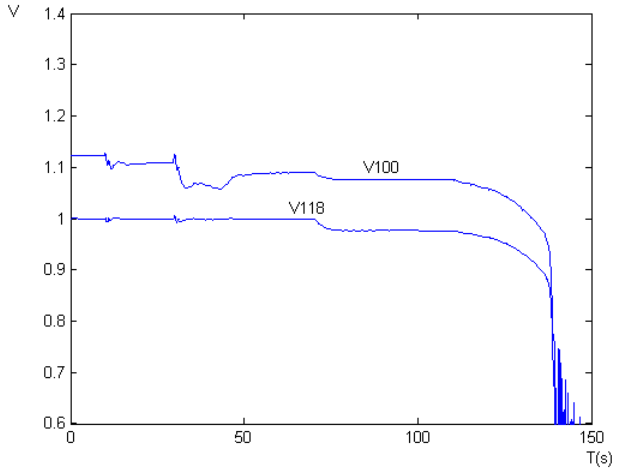

Fig. 1. Voltage profiles at buses 100 and 118

C. *Real and reactive power dynamics*

To clarify the driving force behind voltage instability, the real and reactive power flows are drawn in Figs. 2 and 3. The real power flow does not change much. In Fig. 2, the total real power load in CA is plotted as a solid line, while the dashed line represents the total real power generation in the area. We note that some real power demand is met by real power imports form external areas. Since the trends of changes in real power generation and load are about the same, we note that power flows in tie line between CA sub-area and others remain constant. That means that real power transfers did not change dramatically during this particular voltage emergency. In order to support the same amount of real power loads, the line currents increased when voltages decreased. Therefore, reactive losses were increased and voltage profiles deteriorated.

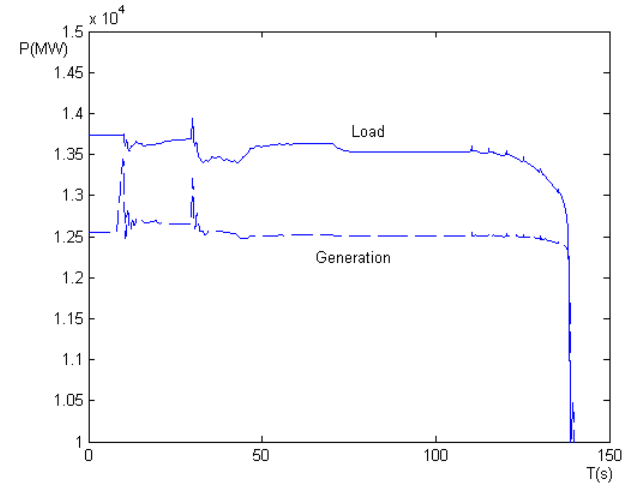

Fig. 2. Active power load and generation in CA

The reactive power flows have a much different behavior that of the real power flows. At the initial operating point, reactive power generations are equal to reactive power demands and reactive power flows in tie lines are almost negligible, which satisfies the economic operation. Reactive power is held in good balance in each sub-area. Following the disturbances, the reactive power flows change dramatically as shown in Fig. 3. Curve 'a' shows the reactive power generation and curve 'b' represents the reactive power demands. Curve 'a' exhibits a significant increase in reactive power generation after 110 seconds. The reactive loads are represented by constant impedance loads and induction motors. The changes in reactive loads are a result of variations in voltages at load buses. The difference between these two plots accounts for transmission reactive losses and shunt capacitor reactive generations. From 50s to 110s, the difference between the two curves remains constant and the system maintains stability. Operations of ULTCs restore voltages and loads on the secondary sides but simultaneously cause voltages on the primary sides and corresponding transmission network voltages to decrease. Deterioration of the system voltage profile has two directly consequences -- reduction of reactive power generations from shunt capacitors and a further increase of transmission reactive power losses. Fig. 4 shows the total reactive power outputs from existing shunt capacitors in the CA sub-area. The significant increase in reactive losses is met by an increase in reactive generation from area generators. Since three generators nearest to affected load area in the middle of CA lose voltage control capability, more distant generators in the area are forced to participate and send the much needed reactive power to the load area. Increase in reactive power flows cause more reactive power losses on transmission lines. The reactive power losses clog reactive power flow to the load area. Meanwhile, generators in external sub-areas outside of CA also begin to participate in this process by supplying additional needed reactive power. Reactive power flows on tie lines are now showing an increase as well.

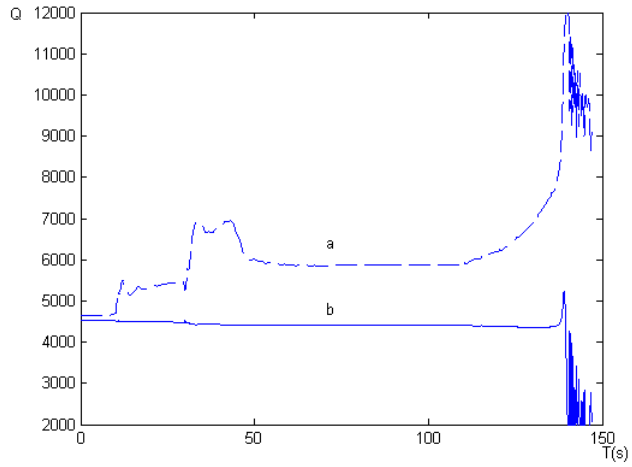

Fig. 3. Reactive power flows in CA

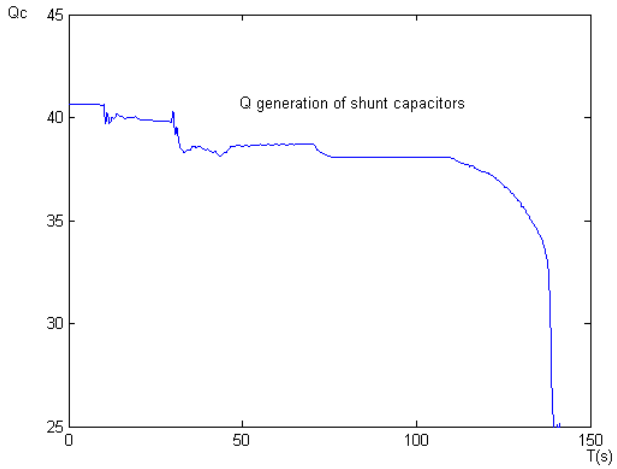

Fig. 4. Reactive power outputs of shunt capacitors

D. *Local and system-wide voltage control*

It is necessary to study system-wide reactive voltage regulation because shortage of reactive power evolves to a

wide-area voltage collapse. The method in [8] is applied to determine voltage control areas and weak areas prone to voltage instability. The reactive power margin in each area may be determined by a QV curve method. Table 1 shows 8 voltage control areas and their margins. The buses and generators within each area are also shown. There is a minimum reactive margin in sub-area 8, which is located in the middle of CA sub-area. This is an indication that the reactive sources are relatively insufficient and this area is prone to voltage instability.

TABLE 1 VOLTAGE CONTROL AREAS

Area	Reactive margin (MVA)	Buses In each area
1	500	2,3,9,12,15
2	1500	12,14,16,19
3	800	50,54,57,58,42,44,46,48,60
4	800	64,142,143,145,146,150,153,143
5	1100	5,8,10,17
6	2300	31,60,74,80
7	350	81,180,86,88,90,89,83
8	200	101,100,113,114,1115, 117,1119

The weakest areas are areas 7 and 8 with reactive margin below 500 Mvar. Generators 144 and 148 are in sub-area 4 in the middle of CA and generator 118 is in sub-area 8 at the top of CA. Due to actions of OELs, a shortage of reactive power happens first in sub-area 4. In Fig. 5, reactive power generations of several generators are shown. The reactive power generations of generators 144 and 148 are limited first at 20 and 40 seconds respectively as shown in Fig. 5(a). Reactive generation is picked up by remote generators, such as generators 118, 116 and 149 in other control areas. The increase of reactive losses is met by these generators also. Then, generator 118 in sub-area 8 exceeds the field current limit at about 70s. Reactive power deficient areas now include sub-areas 4, 7 and 8. After some ULTC operations in these areas, a dramatic increase in reactive losses forces remotely-located generators, such as the generator at 103 to send reactive power.

We note in Fig. 5(b) that the generators increase their reactive power at different rates which depends on electrical distances to the weak areas. Therefore, the loss of voltage control capability in one weak area has a system-wide effect on voltage control. The exhaustion of reactive power reserves in one area can easily lead to depletion of reserves at other areas. During voltage emergencies, all generators participate to counter the reactive power imbalance in the system.

E. Comparison of Static and dynamic methods to find loadability margins

A post disturbance dynamic PV curve [9] is plotted in Fig. 6. Normally, the real power margin can be defined at one bus, one sub-area or the entire system. In this study, the average voltage in CA sub-area is represented as a function of real power loading in the same area. The rate of increase of real load in CA is about 1 MW/second while the reactive load remains constant. Using dynamic simulations by EUROSTAG, the maximum loading in CA was found to be 132 pu.

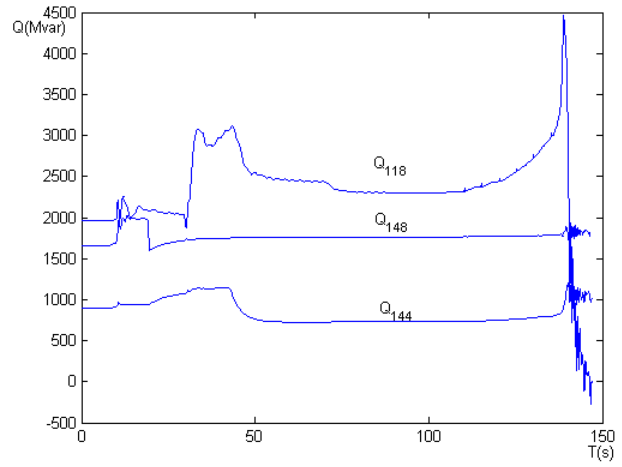

Fig. 5(a). Reactive generation of generators

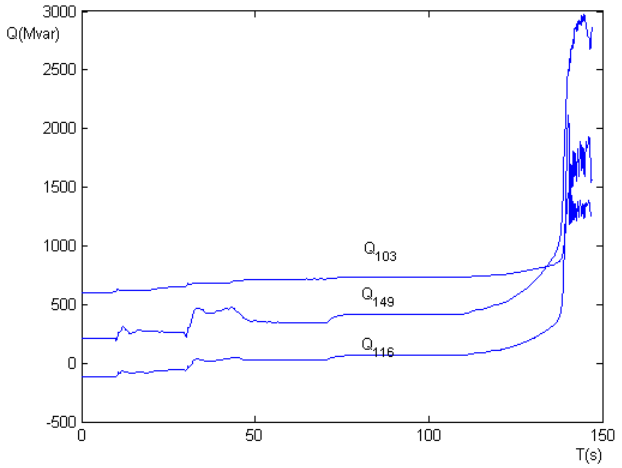

Fig. 5(b). Reactive generation of generators

A second method to determine the maximum loadability is the following: given a real power loading and subject to the above disturbance events, examine system stability using dynamic simulations; then, if the system is stable, increase the loads by a certain percentage and redo dynamic simulations until the system becomes unstable. By following this method, the maximum loading in CA sub-area was found to be 124 pu. The reason for the difference between these two margins is because of the fact that, in the first method, the load increase was only assigned to impendence load.

A third method, the continuation power flow, is used to find the maximum power margin in CA sub-area. This method shows the margin to be 145 pu. These three margins show that the static method is optimistic in evaluating the stability margin.

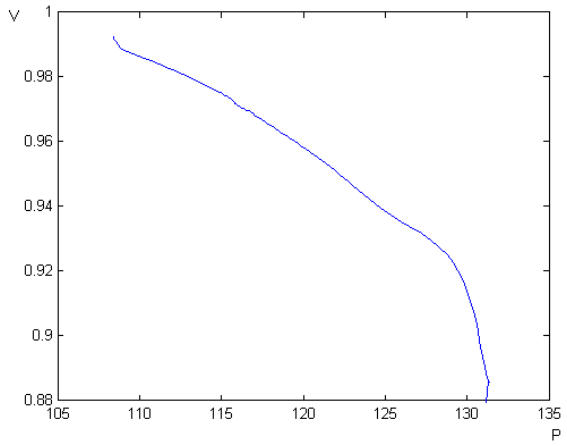

Fig. 6. A dynamic PV curve

F. Effect of load model on voltage stability

Load models play an important role in voltage stability. In the above simulation case, the loads in CA system consist of 50% static loads and 50% induction motors and the system was found to be unstable following the disturbance. If the impedance load was increased to more than 60%, the system survives the same disturbance events. It is obvious that voltage-dependant loads are beneficial to voltage stability. Induction motors have two adverse effects -- the constant real power incurs huge amounts of current flows on the transmission network that cause reactive power loses; and the low voltage may cause induction motors to stall and further increase the reactive load demand. It is critical to model the loads accurately to represent the system.

IV. Corrective Control

The one obvious corrective control strategy is to lock the tap changers from operating in weak areas. In the above simulation case, blocking tap changers can stop the restoration of loads and leave some room to alleviate the system, especially in weak areas where reactive reserves are exhausted.

The second method is to switch shunt capacitors. Since shunt capacitors are slow reactive compensation devices and its reactive generation is dependent on the terminal voltage, the time for shunt capacitors to be engaged is studied in this section. Two shunt capacitor banks are going to be brought on-line during simulations. One bank is at bus 81 in sub-area 7 and another is at bus 1119 in sub-area 8. The compensation amount at bus 81 is 300 MVAR while that at bus 1119 is 200 MVar. In case 'a' the shunt banks are switched on at 100 seconds while, in case 'b,' they are turned on at 130 seconds. The two operation schemes result in two different consequences as shown in Fig. 7. In case 'a,' switching on the shunt capacitor prevents the system from collapse. In case 'b,' it seems that the shunt capacitor cannot stop the voltage instability from occurring. It is of utmost importance to coordinate compensation switching times with respect to the maximum time available before system collapses. Also, a single shunt capacitor switched on at either bus 81 or bus 1119 cannot prevent the system from collapsing, with any practical amount of reactive output.

These simulations show that local voltage control may not be enough to prevent voltage instability and that coordination of controls at different voltage control areas may be necessary. Besides, time dependency of controls is an important factor to consider.

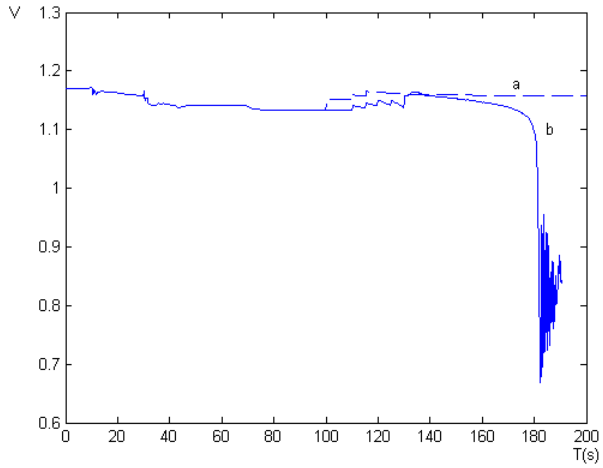

Fig. 7. Bus voltage trajectories at bus 1119 with different shunt switching schemes

V. Conclusions

This paper presents a dynamic analysis of voltage collapse. Some conclusions may be drawn based on the above analysis.

1. System-wide reactive power monitoring provides a good signal for voltage stability control design. Reactive power losses clog reactive power flow to the load area and may eventually lead to system collapse.
2. Voltage reactive control function of generator is system-wide -- exhausting reactive power reserves in one area may easily lead to depletion of reserves in other areas.
3. The static method is optimistic in evaluating stability margins.
4. Different load models may change the nature of stability of the system.
5. Coordination of preventive controls in several voltage control areas may be necessary. Controls may also be time-dependent.
6. In the open access environment, providing necessary voltage stability support should become part of any large power transfers or wheeling services.

VI. References

[1] NERC, "Survey of the Voltage Collapse Phenomenon," *Technical Report North American Electric Reliability Council*, 1990.

[2] B. Gao, G.K.Morrison, and P. Kundur, "Voltage stability evaluation using modal analysis," *IEEE Trans. Power Systems*, vol. 7, no.4, November 1992, pp:1529-1542.

[3] V, Ajjarapu, and C Christy, “The continuation power flow: A tool for steady state voltage stability analysis,” *IEEE Trans. Power Systems*, vol. 7, no.1, February 1992, pp: 416-423.
[4] Garng Huang; H. Zhang, “Dynamic voltage stability reserve studies for deregulated environment,” *IEEE Power Engineering Society Summer Meeting*, 2001, Vancouver, Canada, 15-19 July 2001.
[5] T. Tran-Quoc, T. Vu-Duc, R. Feuillet, N. Hadjsaid, J.C. Sabonnadibre, C. Praing, L. Tran-Dinh, “Dynamic analysis of voltage instability in the Vietnam system,” *Proc. International Conference on of EMPD '98*, March 1998.
[6] Tractebel Enginering, *EUROSTAG manual*. May 1999.
[7] C. W. Taylor, *Power System Voltage Stability*, McGraw-Hill, Inc. 1994.
[8] R.A. Schlueter, "A voltage stability security assessment method," *IEEE Trans. Power Systems*, Vol. 13, No. 4, pp. 1423 -1438, Nov. 1998.
[9] F. Dong, B.H. Chowdhury, M.L. Crow, L. Acar, “Further Investigation of Static and Dynamic “P-V Curves” for Voltage Stability Assessment,” *North American Power Sym.*, Texas A&M Univ., College Station, TX, Oct., 2001.

Appendix

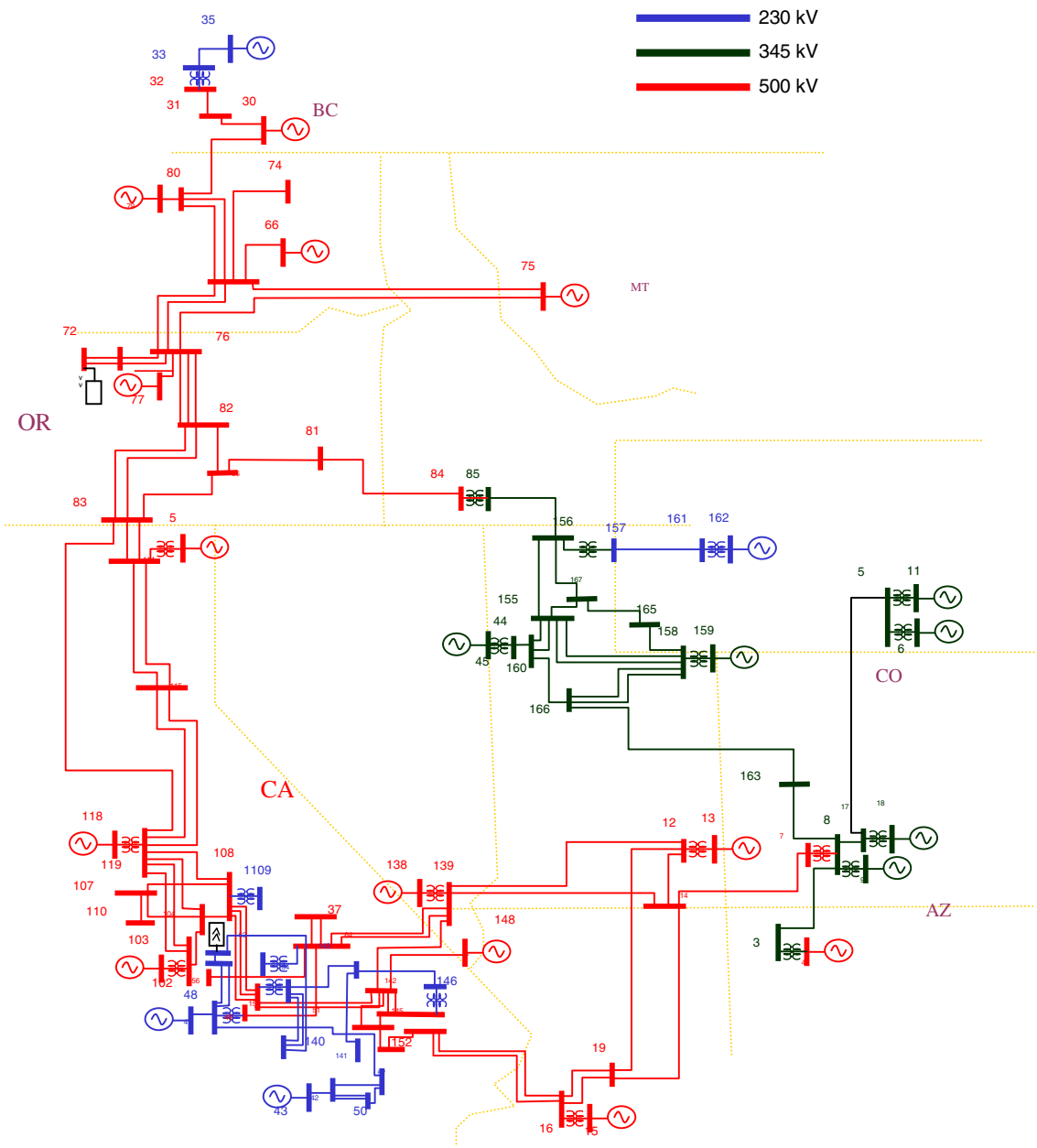

VII. BIOGRAPHIES

Feng Dong received his BS and MS degrees in Electrical Engineering from Hohai University, Nanjing, China, respectively in 1995 and 1999. He is presently a Ph.D. student at the Department of Electrical Engineering, University of Missouri-Rolla.

Badrul H. Chowdhury obtained his M.S. and Ph.D. degrees in Electrical Engineering from Virginia Tech, Blacksburg, VA in 1983 and 1987 respectively. He is currently a Professor in the Electrical & Computer Engineering department of the University of Missouri-Rolla.

Mariesa L. Crow received her BSEE from the University of Michigan and her Ph.D. from the University of Illinois – Urbana/Champaign in 1989 both in Electrical Engineering. She is currently Associate Dean for Graduate Studies and Research and a Professor of Electrical and Computer Engineering.

Levent Acar obtained his M.S and Ph.D degrees in Electrical Engineering from The Ohio State University, Columbus, OH in 1984 and 1988 respectively. He is currently as Associate Professor in the ECE Department at UMR.